Journal of Non-Newtonian Fluid Mechanics, 21 (1986) 337–358
Elsevier Science Publishers B V, Amsterdam – Printed in The Netherlands

EXPERIMENTAL VELOCITY DISTRIBUTION MEASUREMENTS OF HIGH DENSITY POLYETHYLENE FLOWING INTO AND WITHIN A SLIT

M.R MACKLEY and I P T MOORE

Department of Chemical Engineering, University of Cambridge, Pembroke Street, Cambridge, CB2 3RA (Gt Britain)

(Received July 30, 1985, in revised form February 7, 1986)

Summary

Using the Laser doppler technique we report experimental velocity profile measurements of molten polyethylene flowing into a slit die. Our experimental measurements are restricted to the centreline of the flow and three transverse sections within the slit. The results indicate that with the exception of a high flowrate centreline velocity overshoot, the normalised velocity profiles are relatively insensitive to both temperature, polymer grade and flowrate.

We have also carried out an analysis and simulation to establish the effect on velocity measurements of both velocity gradients and solid boundaries within the probe volume of the intersecting laser beams used to measure the velocity profiles. Our results indicate that for our own experimental conditions we might expect to measure a finite velocity at the wall and that the presence of velocity gradients will not significantly effect the time dependence of the auto correlogram.

1. Introduction

The main objective of this paper is to report experimentally determined velocity profile measurements of molten polyethylene flowing into a slit die. In particular, we concentrate on the behaviour of the centreline velocity profile as a function of mean flowrate, temperature and polymer grade. In a companion paper to this one [1] we use the kinematics for the velocity profile given her, together with an appropriate constitutive equation and polymer properties in order to simulate the associated centreline stress

0377-0257/86/$03 50

distribution. This stress distribution can then be compared with that observed experimentally from flow birefringence observations.

Velocity measurements can be made in any transparent fluid by detecting the Doppler shift in the frequency of light scattered by particles in the moving fluid. If the scattering region is defined by the intersection of two laser beams the frequency of the scattered light is independent of the direction of scattering and is sufficiently low to measure using photon counting methods. Laser-Doppler velocimetry based on these principles has been applied to measurements in a variety of flows in open air and in restricted spaces. The main advantage for the latter type of application is that the method is non-intrusive and the measuring region can be defined very precisely The use of laser-doppler velocimetry for measurements on polymer melts has been limited, despite its obvious advantages. Kramer and Meissner [2] have reported velocity profiles for molten low-density polyethylene flowing into an abrupt contraction in a square section tube using a laser-doppler velocimeter arranged in a backward scattering mode, and a number of authors [3–5] have made measurements on flowing polymer solutions using similar systems.

The most popular method in the past for velocity measurements in molten polymers has been streak photography which has been described by amongst others Drexler and Han [6,7]. The drawback of this method is that, as the velocity increases, the exposure time must be reduced to maintain positional accuracy. Eventually a limit is reached, either due to weakness of the illumination or due to the minimum exposure time of the camera. The compensating advantage is that the apparatus is simple compared to a laser-Doppler velocimeter and relatively insensitive to operating conditions. The laser-Doppler system has to be aligned with care and can be affected by stray reflections of light from, for example, the windows around the sample.

This paper and its companion [1] consider in detail the flow on the centreline of a rectangular duct. This is an extensional shear flow in which

$$\dot{e} = \frac{\partial V_1}{\partial x_1} = -\frac{\partial V_2}{\partial x_2}.$$

Such flows are important in many processing operations such as fibre drawing and die extrusion, but measurement of material properties in extensional flow is difficult, particularly at extension rates typical of industrial processing.; Methods which have been used include stretching rods of molten material [8–10] and, for less viscous materials, suspended syphon flow [11,12] and the triple jet [13]. An alternative, suggested by Cogswell [14] among others, is to use a controlled convergent geometry and measure both stresses and strain rates. This paper demonstrates that the latter can readily be achieved using laser-doppler velocimetry whilst the companion paper [1]

confirms that the same basic apparatus can also be used for stress measurements, thus bringing a new type of converging flow extensional rheometer close to fruition.

2. Experimental details

The layout of the experiment is shown in Fig. 1. The extruder is a Betol 2520J single screw extruder with a 25-mm barrel exit. A calming section was inserted between the barrel and the die section to allow the flow pattern to develop and, by means of extra heating elements, to allow the temperature of the polymer melt to be "fine tuned" to match that of the die. The die section and the block in which it is mounted are shown in detail in Fig. 2. 1.5-cm-thick strain-free glass windows on either side of the die permit the flow in the die to be observed in detail. In order to seal the windows around

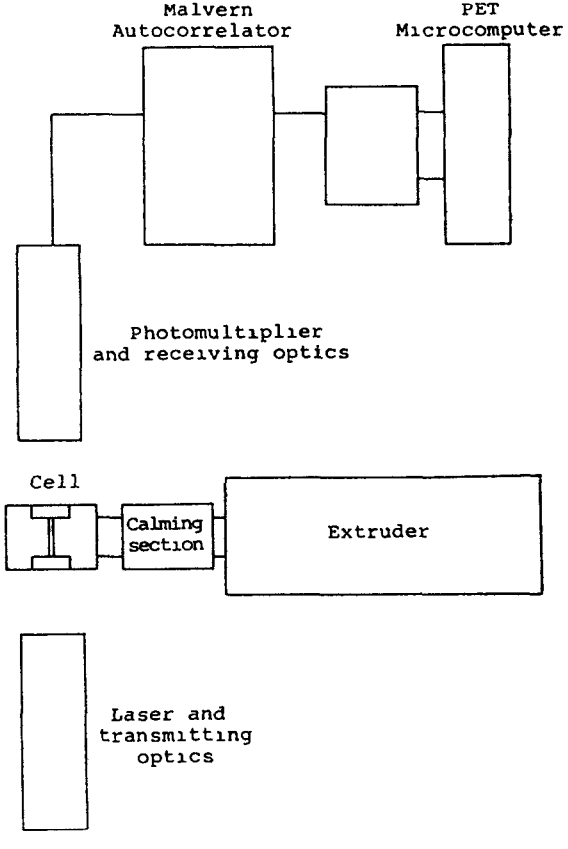

Fig 1 Schematic diagram of apparatus

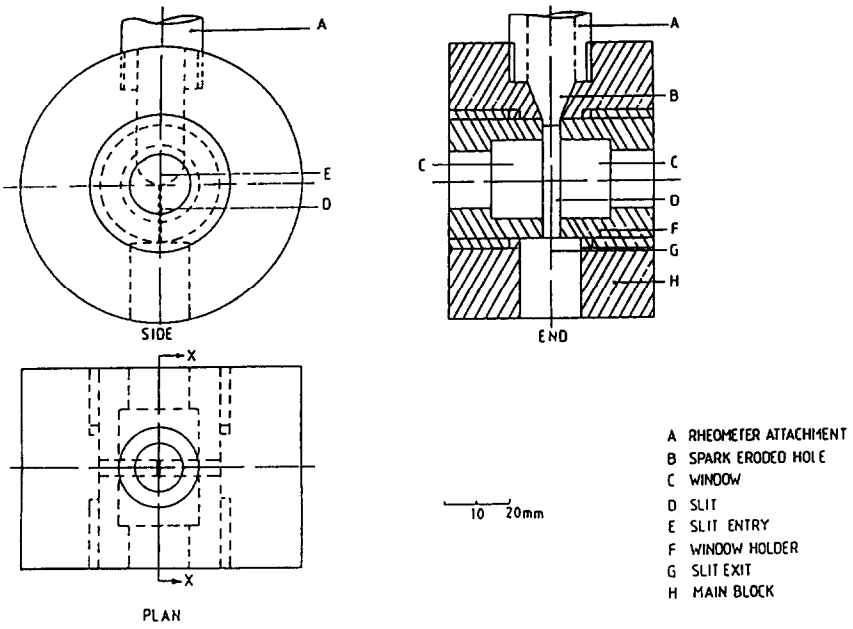

Fig 2 Geometrical drawing of die assembly

the die without imposing undue strain on them, a threaded mount fastens into the block with a high temperature washer to hold the window. The block is heated by two 375 W band heaters which allow its temperature to be controlled to $\pm 1°C$. Thermocouple insertion points around the block were used to check that a uniform temperature was achieved. The die chosen for this work was a rectangular slit section 1-mm wide by 7.6-mm deep as shown in Fig. 3. The upstream approach is semicircular, which gives a sharp entrance to the die but eliminates for high density polyethylene the recirculation zones often observed in an abrupt contraction [15,16].

The arrangement of the measuring system for laser doppler velocimetry is shown schematically in Fig. 4. The shelf mounted on the lathe bed provides a rigid support for the laser and its receiving optics which are arranged in forward-scatter mode Two crossheads fixed to the lathe bed allow the shelf to be traversed accurately parallel to the axis of the die, and across its width. The same shelf was also used as a mounting for the optical equipment used in flow birefringence measurements whose results are described in a companion paper [1]. The aspect ratio of the slit, and its narrow width places carious constraints on the use of the laser-Doppler velocimeter In order to obtain high spatial resolution it is necessary to first expand the laser beam to approximately 1 cm diameter and then focus the expanded beam using a

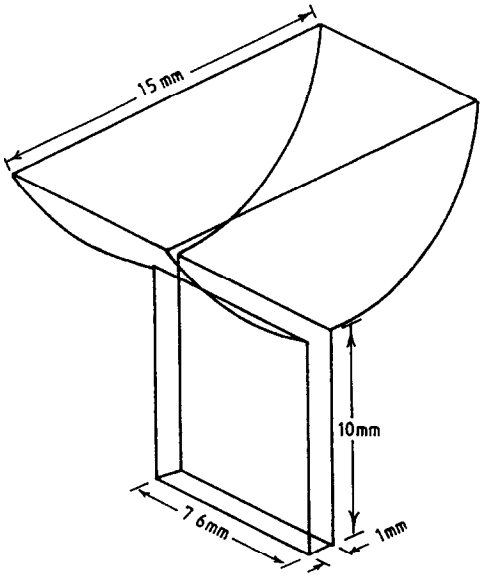

Fig. 3 Dimensions and shape of duct

20-cm focal length lens. This gives a final minimum beam radius at the intersection waist of approximately 5 μm and the beam splitter is arranged so that the beams cross over at the waist. The focussing of the beams results in a sample region (the region where the beams intersect) with a complex shape, but the aspect ratio of the slit is such that the long dimension of the sample region is relatively unimportant. With such good spatial resolution

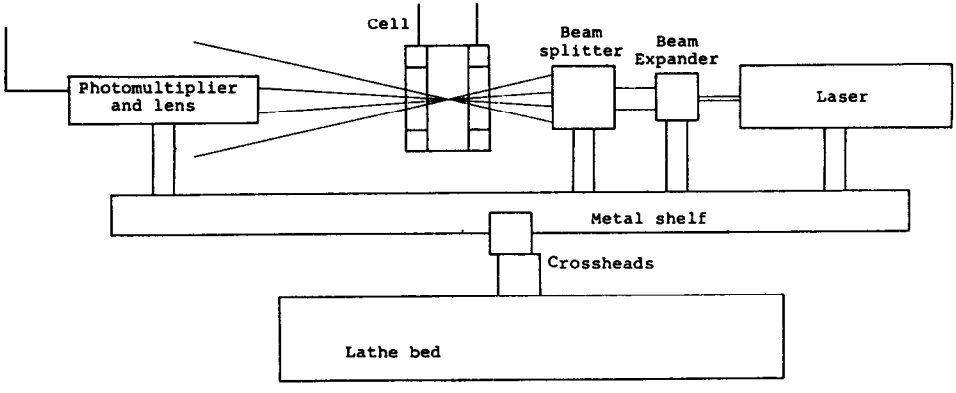

Fig 4. Schematic diagram of laser optics

(typically 40 μm) it is essential that the sample region be correctly positioned within the slit and to do this the points at which the slit walls interrupt the beam on either side are found, and the centreline taken to be midway between these points.

The receiving optics consist of a photomultiplier tube and a photographic lens. The lens is focussed on the sample region and a pinhole is used to cut out light from other sources (such as reflections from the transmitted laser beams). The output from the photomultiplier is analysed using a Malvern Instruments K7025 Photon Correlator. This correlates the signal from the photomultiplier in a short time period (typically 100–1000 ns). Any periodic component of the signal then appears in the "autocorrelation function" generated by the system, as a decaying cosine wave. This process has been described in more detail by several authors [17,18]. A summary of how the autocorrelation function is generated is given in Appendix 1.

3. Effect of velocity gradients and walls on velocity measurement

The velocity autocorrelation function (a.c.f.) as shown in Appendix 1 is a function of all the velocities present in the sampling region during a

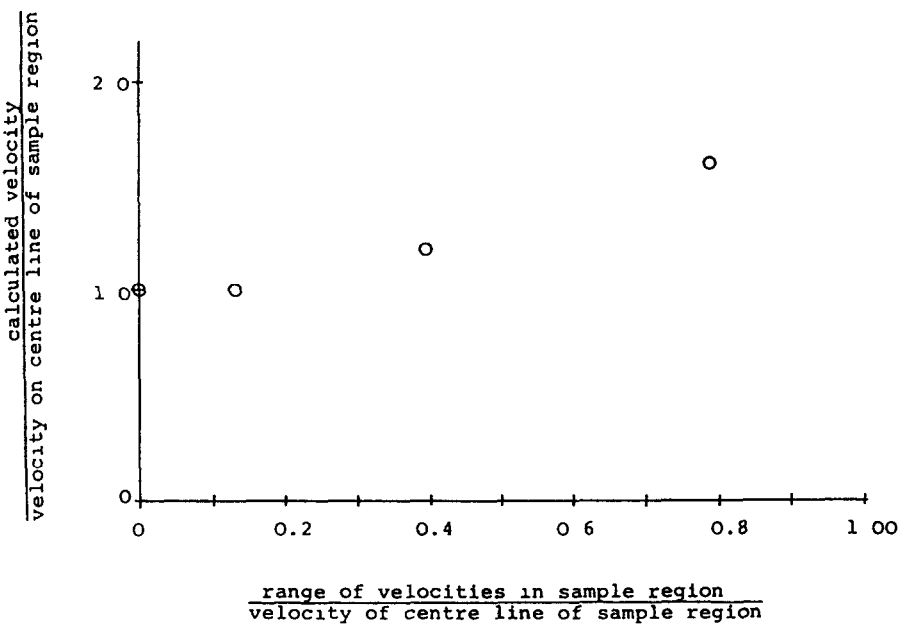

Fig 5 Graph showing the ratio of calculated velocity/centre velocity, as a function of maximum velocity range/centre velocity

measurement. It is possible to analyse the a.c.f., using a Fourier Transform for example, and extract the velocity distribution, and this facility is available on the more recent Malvern Velocimeters [19]. However, the early model described here only indicates "turbulence intensity" based on an assumption of a Gaussian velocity distribution, which is of little interest when considering the laminar flow of molten polymers. Two effects which could occur in

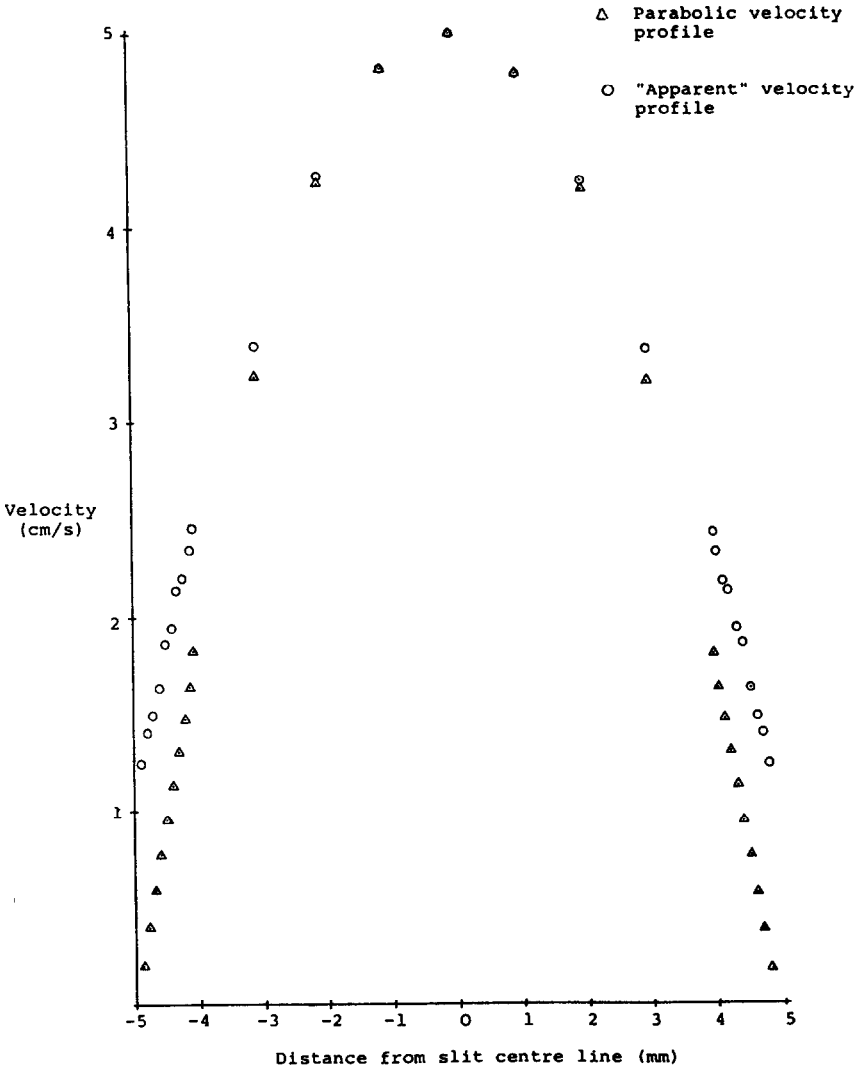

Fig. 6 Diagram showing the effect of beam cut off at the wall ▲ model parabolic velocity profile ⊙ velocity profile predicted using equation (A4).

such flows were investigated as part of this work, to ensure that no distortion would be introduced to the velocity measurements. These were the effect of very high velocity gradients (giving a wide spread of velocities in the sample region) and the effect of part of the sample region being blocked by the slit wall (so that the mean velocity measured was no longer in the centre of the sample region). The mathematical treatment of the autocorrelation function used in modelling these two cases is given in Appendix 1. The results of the model for the effect of velocity gradients are shown in Fig. 5. The a.c.f. for a uniform velocity across the sample region is compared with those for increasing velocity gradients (equivalent to increasing the range of velocities sampled). As can be seen, the apparent mean velocity is only affected when the range of velocities sampled exceeds 10% of the mean value in the sample region. With the small sample region used in the experiment there is unlikely to be any region where the velocity gradient is sufficiently large to give this effect. The second effect studied was that resulting from partial obscuration of the sample region by the slit wall. In this case the results are best illustrated by Fig. 6, which shows a parabolic velocity profile across the slit and the predicted velocity profile that would be obtained using a laser doppler system with a 67-μm beam radius to measure the parabolic profile. The profile which one might expect to measure is significantly distorted and has a finite velocity at the wall which was not present in the parabolic profile used to generate it. Again, the effect would be reduced by using a smaller beam radius but, in this case, care would be necessary since the focussed beam is wider at the windows than in the sampling region.

The main conclusion from this simulation work is that the measuring system used in these experiments should not introduce any significant distortions into the results. However, if a laser doppler velocimeters is to be used in a confined region, the effects of high velocity gradients and of obstruction of the beams by the walls must be considered.

4. Velocity measurements

Velocity measurements were made in the apparatus described, using molten high-density polyethylene. Two grades of BP Chemicals Rigidex polymers were chosen (140-60 $M_n = 14000$, $M_w = 65000$ and 006-60 $M_n = 20000$, $M_w = 130000$). These materials are highly transparent when molten and it was necessary to add seed particles to ensure a sufficient level of light scattering for the velocimeter. Approximately 0.2% w/w of 0.5–5 μm molecular sieve (sodium aluminosilicate) was shaken with the polymer granules before filling the feed hopper of the extruder and this adhered to the surface of the granules giving an even distribution after melting. The

measurements on each polymer were made at a number of volume flowrates and several temperatures. As far as possible these were matched, but control of the extruder was by screw speed so flowrates are rarely exactly equal in

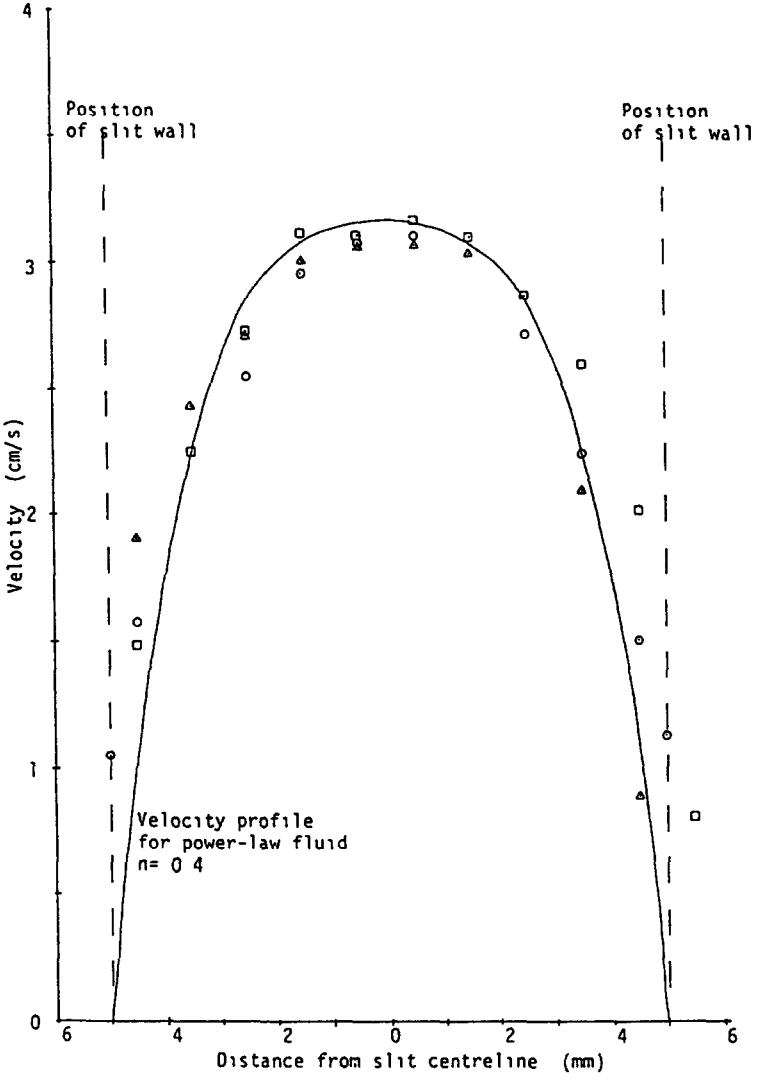

Fig 7 Transverse velocity profiles across slit for HDPE 006-60 at 210°C (Run 8). Distance downstream from throat ▲ 0 1 mm, ⊡ 2 0 mm, ⊙ 6.0 mm Continuous curve represents velocity profile of power-law fluid with power-law index $n = 0\,4$

different runs. Figure 7 shows velocity profiles measured across the width of the slit at various points along its length, using 006-60 at 190°C. Only the one set of transverse velocity profiles was measured, but it illustrates several important points. Firstly, the velocity profile across the slit matches reasona-

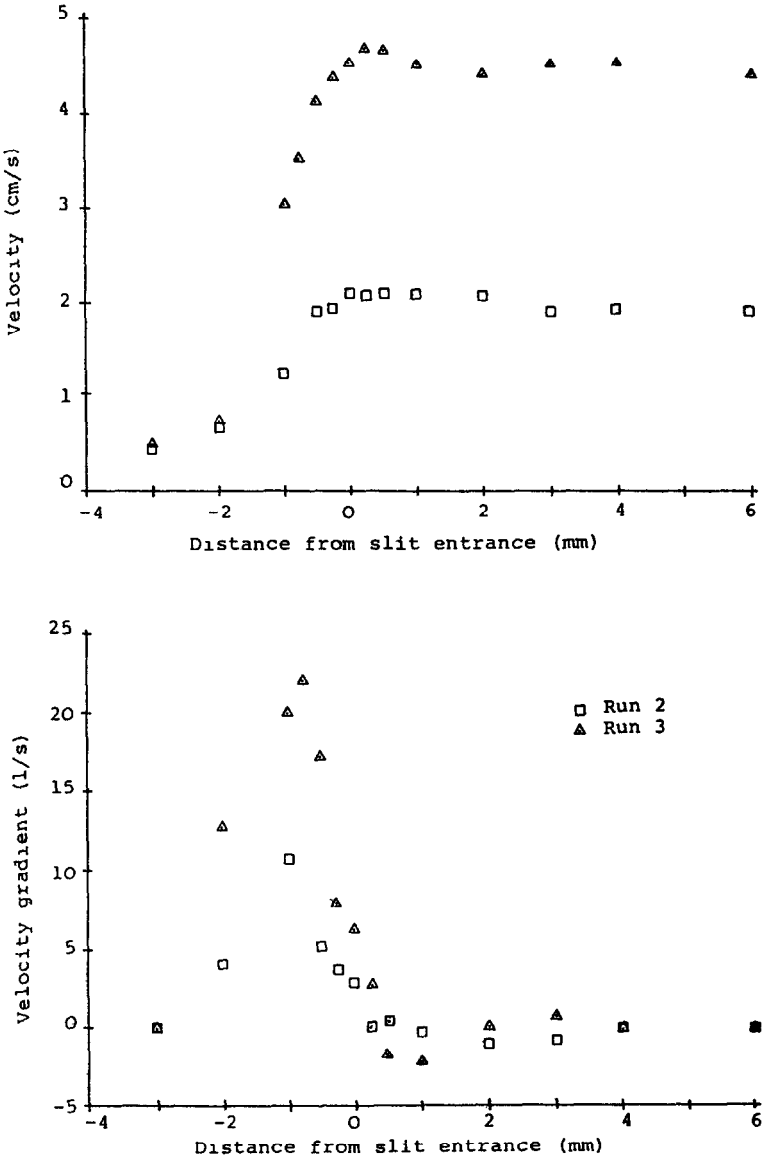

Fig 8 Centreline velocity and velocity gradient data for HDPE 006/60 $T = 170°C$ see Table 1 for details

bly that predicted for a power-law fluid (i.e. one for which the apparent viscosity η is given by $\eta = k\dot{\gamma}^{n-1}$) where $n \simeq 0.4$ and this power law index is in reasonable agreement with the expectations for 006-60. There is some

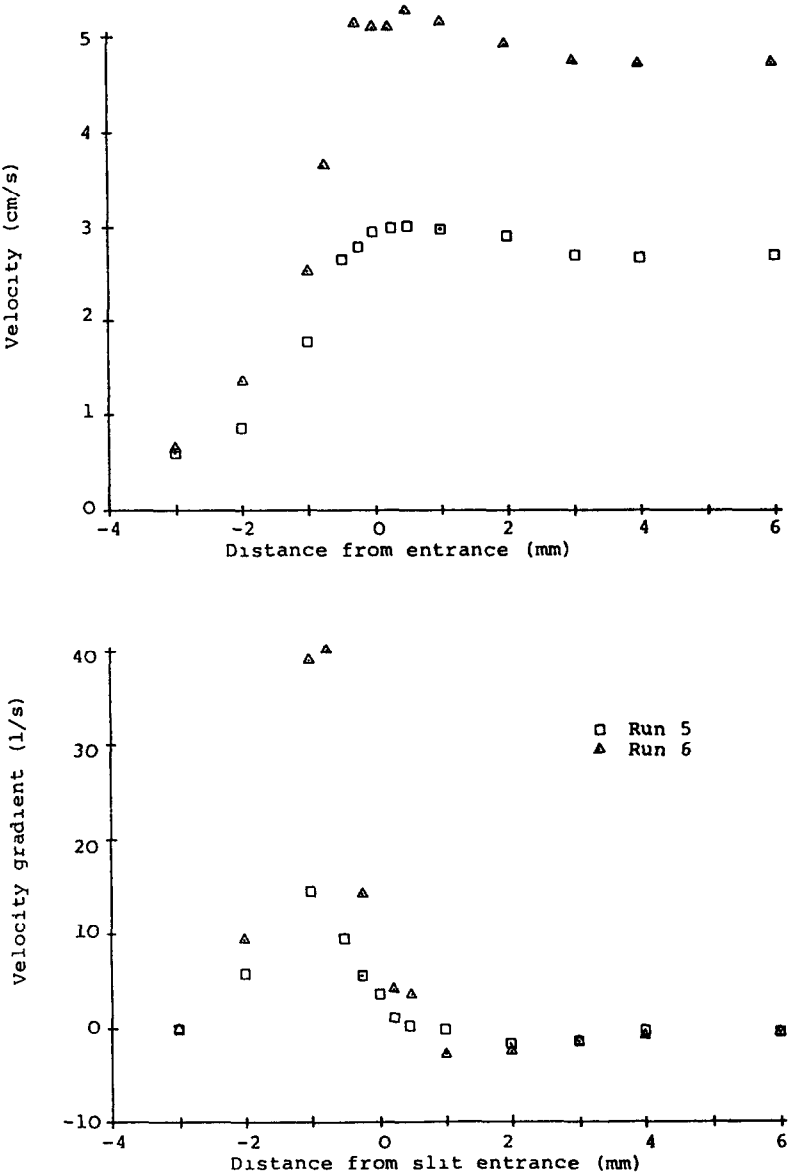

Fig 9 Centreline velocity and velocity gradient data for HDPE 006/60 $T = 210°C$ see Table 1 for details

slight deviation from the prediction close to the slit wall and an apparent finite velocity at and even within the wall. This latter observation can be explained by the beam cut-off effect discussed in the preceding section. The

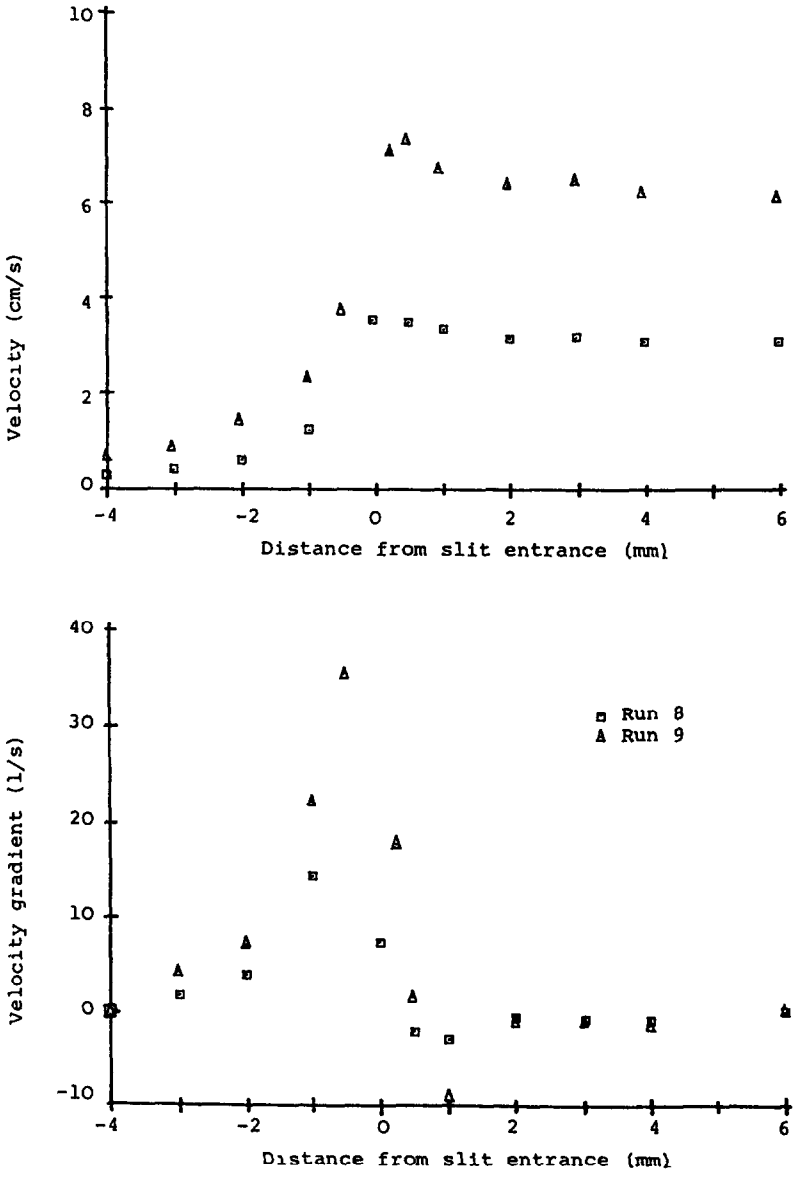

Fig. 10. Centreline velocity and velocity gradient data for HDPE 006/60. $T = 210°C$ see Table 1 for details.

only way in which a velocity can be measured inside the solid wall is if it occurs as an artefact of the measuring system and it is reasonable to assume that the same applies to velocities at the wall. The second notable point is

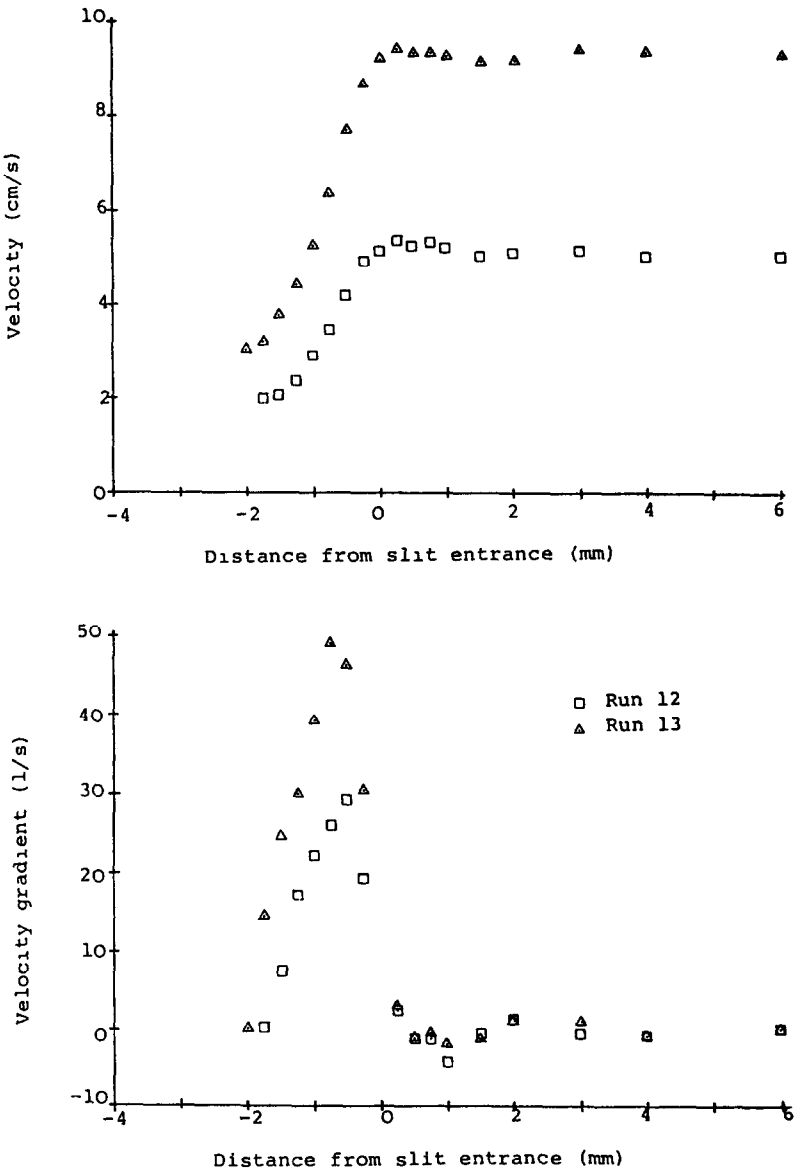

Fig 11 Centreline velocity and velocity gradient data for HDPE 140/60. $T = 150°C$ see Table 1 for details

that the velocity profiles are almost identical at the three sections down the slit. This shows that the development of the flow within the slit occurs very rapidly downstream of the throat, particularly as one profile was measured only 0.1 mm downstream. This observation has been predicted [20] for

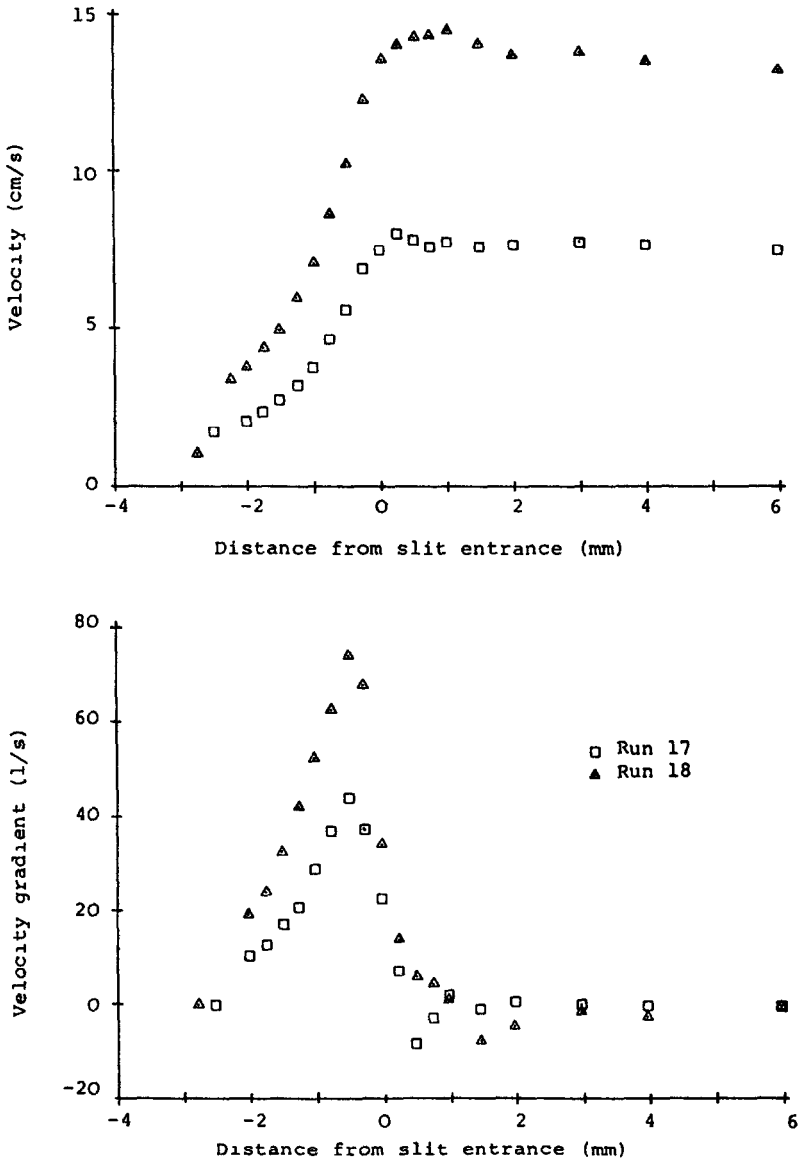

Fig 12. Centreline velocity and velocity gradient data for HDPE 140/60. $T = 170°C$ see Table 1 for details

Newtonian fluids of a similar viscosity and is important when considering the relaxation of stresses down stream of the entrance, as we do in [1].

Figures 8 to 13 shows the measured velocity profiles along the centre line of the slit for the two grades of H.D.P.E. at various overall flowrates and

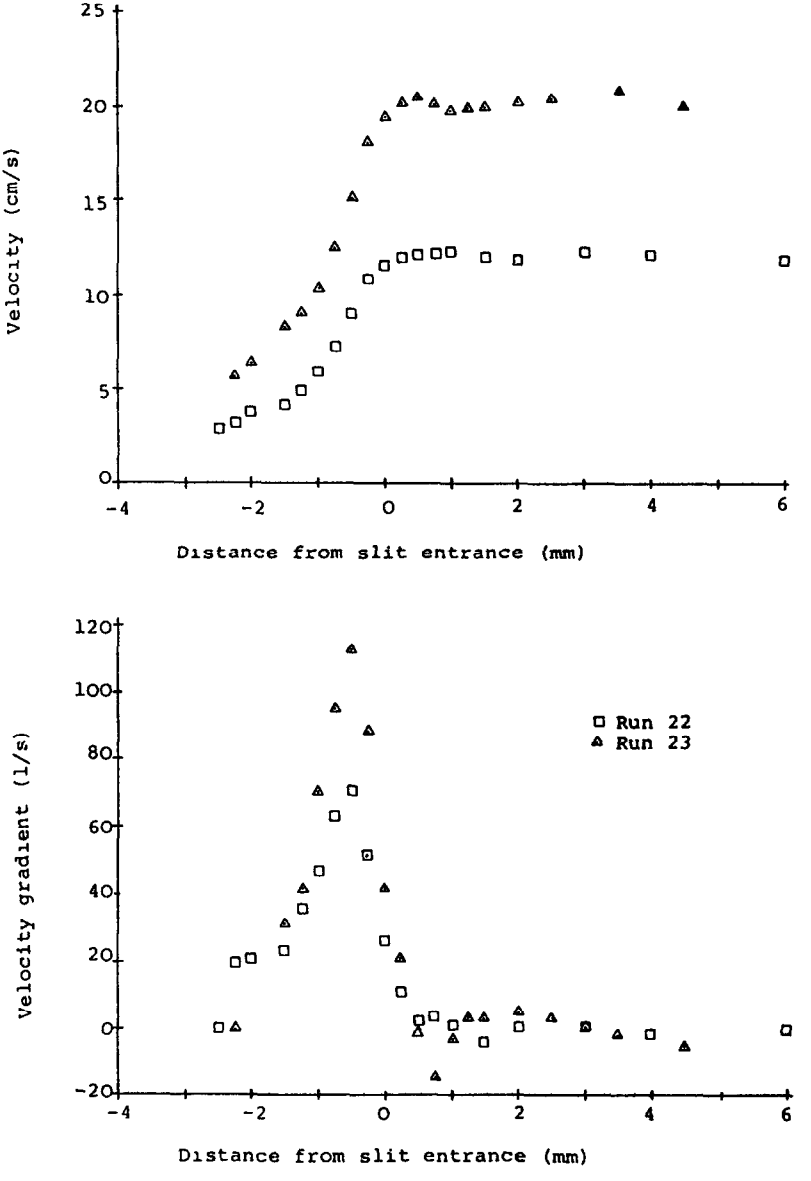

Fig 13. Centreline velocity and velocity gradient data for HDPE 140/60 $T = 170°C$ see Table 1 for details

TABLE 1

Data relating to Figs. 8–13

Figure number	Material	Temperature °C	Run number	Maximum entry velocity gradient e_m (s^{-1})	Centreline velocity within slit v (cm/s)
			2	14	2 0
8	HDPE	170	3	22	4 5
	Rigidex 006-60		5	15	2 8
9	$m_w = 20000$	190	6	40	4 8
	$m_w = 130000$		8	15	3 2
10		210	9	35	6 4
			12	29	5 1
11	HDPE	150	13	49	9 3
	Rigidex 140-60		17	44	7 7
12	$m_n = 14000$	170	18	74	13 8
	$m_w = 65000$		22	71	12 4
13		190	23	113	20 4

different temperatures. The figures also show the velocity gradient profiles, calculated from the velocity data using a simple quadratic curve-fitting algorithm. Details of the processing conditions are given in Table 1 and the linear viscoelastic behaviour of both polymers is also given in Fig. 3 of [1].

We estimate an accuracy in our velocity measurements of order $\pm 10\%$ however the uncertainty increases as velocity measurements are made near walls and when extruder flowrates are high. Generally centreline velocity profile measurements presented little difficulties once the optics were set up correctly. Eash measurement recorded in the figures was an average of five velocity measurements taken at that point and we attribute most of the velocity fluctuations to time-dependent flow variations from the extruder.

The major features of the centreline velocity profiles can be described as follows. The individual velocity profiles all show a very sharp acceleration of the flow in the region just upstream of the entrance, followed by an almost constant velocity in the slit. The acceleration occurs over a very small distance (approximately four slit widths) and, as can be seen from Figs. 14 and 15 which show the velocity profiles normalized in terms of the velocity in the slit, the profile is similar under all conditions. The velocity on the centreline within the slit well down stream of the throat is approximately constant for each run, as was suggested by the profiles across the slit shown in Fig. 7. Figure 7 also indicates that the velocity profile across the slit is

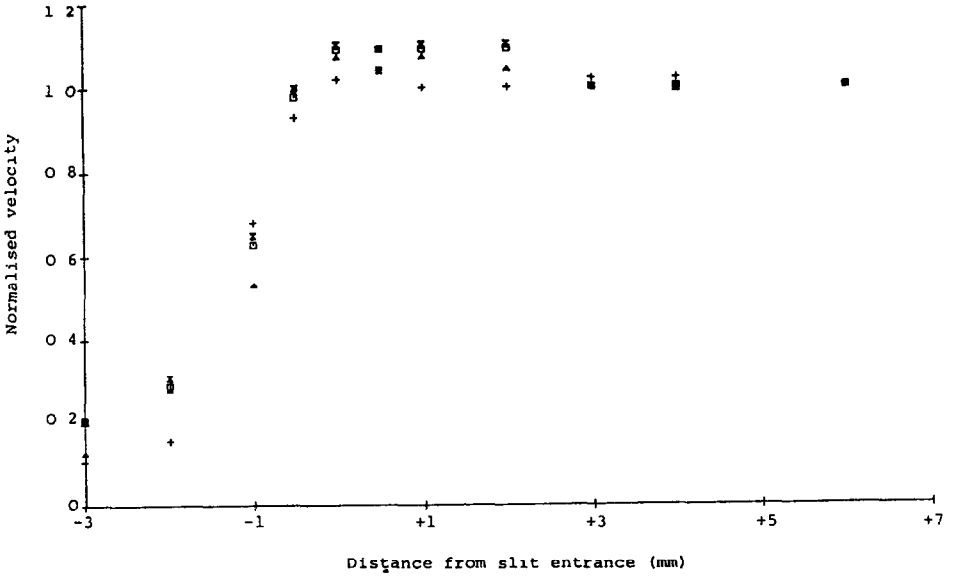

Fig 14. Normalized velocity profiles for HDPE 006/60 + run 3, ⧖ run 2, ▲ run 6, ⊡ run 5 see Table 1 for details

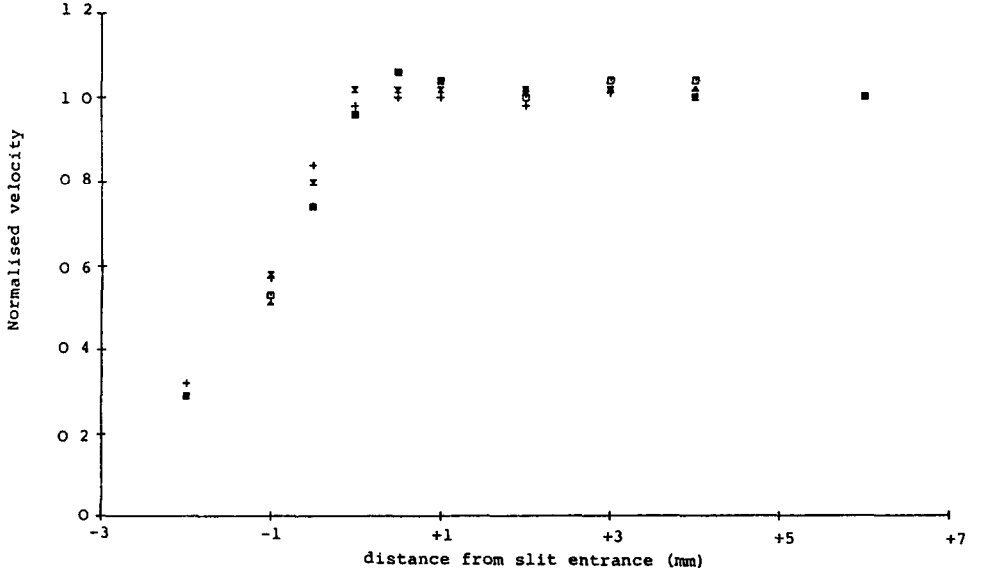

Fig 15 Normalized velocity profiles for HDPE 140/60 + run 13, ⧖ run 12, ▲ run 18, ⊡ run 17 see Table 1 for details

sufficiently flat in the central region that slight misalignment of the measuring system relative to the slit axis will not affect the validity of the results. The variations in the velocity measured in the slit that can be seen in the normalised profiles (Figs. 14 and 15) are due to fluctuations in the mass flowrate from the extruder. These fluctuations were as high as $\pm 5\%$ of the total flow and could not be explained, except by assuming that the screw speed was varying.

Immediately downstream of the throat the velocity on the centreline appears to go through a maximum, which becomes more apparent with increasing flowrate. This velocity "overshoot" has been predicted for elastic liquids flowing into a sudden contraction [21] and has been observed by other workers using geometries of that type [2,3] The unusual shape of the die entrance in these experiments has not been modelled, but the observation suggests that the "overshoot" is due to the sharp-cornered entrance and not, as has been suggested, to the recirculating flows present in some sudden contractions.

An important result, which can be seen from the normalized profiles, is that the shape of the velocity profile on the centreline in the slit and in the entrance region, is relatively independent of flowrate, temperature and molecular weight, as least over the range of these variables considered. This suggests that, under the conditions of these experiments, the flow pattern is determined more by the shape of the duct than by the material properties. Again, numerical models of the flow in an abrupt contraction indicate that this should occur in creeping flow [20].

5. Conclusions

Our autocorrelation simulations have shown that for the experimental conditions used in this paper the presence of velocity gradients will not have a significant effect on the mean velocity measurements that we make at any one spatical position. The simulations do indicate that we should expect to record a finite velocity at the wall even if the fluid velocity there is zero and this result was confirmed by our experimental measurements of the transverse profiles within the slit.

Within the slit and downstream of the throat we observe the rapid development of a steady transverse velocity profile consistent with that of a power-law fluid, this in turn is entirely consistent with expectations for a high viscosity flow with Reynolds number Re of order 10^{-4}. Upstream of the throat the centreline velocity changes occurred typically over distances of three to four slit widths and these changes were relatively independent of polymer grade and or temperature. At higher flowrates a velocity overshoot was observed on the centreline immediately downstream of the throat,

however the generally observed characteristic feature within the slit section was that the centreline velocity remained essentially constant for all polymers, temperatures and at any given flowrate as the fluid moved within and along the centreline of the slit.

Acknowledgements

We would like to acknowledge both SERC and BP Chemicals Limited for their financial support of this work. In addition we thank Mr John Pryor from this department for his skillful construction of many parts of the apparatus.

References

1 S T E Aldhouse, M R Mackley and I P T Moore, J Non-Newtonian Fluid, 21 (1986) 359–376
2 H Kramer and J Meissner, Proc 8th Int Congr Rheol, Plenum, 1980
3 E D Pashkin, Fluid Dynamics, 15 (1976) 358
4 E.T Busby and W C MacSporran, J Non-Newtonian Fluid Mech, 1 (1976) 71
5 T Cochrane, K Walters and M F Webster, J Non-Newtonian Fluid Mech, 10 (1982) 95
6 L H Drexler and C D Han, J Appl Polym Sci, 17 (1973) 2329
7 L H Drexler and C D Han, J Appl Polym Sci, 17 (1973) 2355
8 J Meissner, Trans Soc Rheol, 16 (1972) 405
9 H Munstedt, J. Rheol, 23 (1979) 421
10 Sangamo Schlumberger, Elongational Viscometer, Bognor Regis, Sussex, UK
11 G Astarita and L Nicodemo, Chem Eng J, 1 (1970) 57
12 W C MacSporran, J Non-Newtonian Fluid Mech, 8 (1981) 119
13 D R Oliver and R Bragg, Chem Eng J, 5 (1973) 1
14 F N Cogswell, J Non-Newtonian Fluid Mech., 4 (1978) 23–38
15 T H Nguyen, Ph D Dissertation, Monash University, 1978
16 J L White and A Kondo, J Non-Newtonian Fluid Mech, 3 (1977/78) 41
17 L R Dram, The Laser Doppler Technique, Wiley, 1980
18 E R Pike, Photon correlation velocimetry in photon correlation spectroscopy and velocimetry in H Z Cummins and E R Pike (Eds) Plenum, 1980, p 246
19 Malvern Instruments K 7027 Photon Correlation Technical Information Sheet
20 J R Black, M M Denn and G C Hsiao, in Theoretical Rheology, J F Hutton, J R A Pearson and K Walters (Eds), Applied Science Publishers, 1975, p 3
21 M Viriyayuthakorn and B Caswell, J Non-Newtonian Fluid Mech, 6 (1980) 245
22 J B Abbiss, T W Chubb and E R Pike, Optical and Laser Technol, December 1974, p 149

Appendix 1

The autocorrelation function

The intensity of light scattered by a particle passing through the intersection of two laser beams is given by [18]

$$I(T) = I_0 \exp\left(\frac{-2u^2(T-t_0)^2}{r^2}\right)\cos^2\left(\frac{\pi u(T-t_0)}{s}\right) \tag{A1}$$

where I_0 is the intensity at the centre of the sample region, which the particle crosses at time t_0. u is the particle velocity and s the fringe spacing. The exponential term allows for the Gaussian intensity distribution across the laser beam and the cosine term can be visualised in terms of the particle crossing a series of interference fringes in the intersection of the two beams.

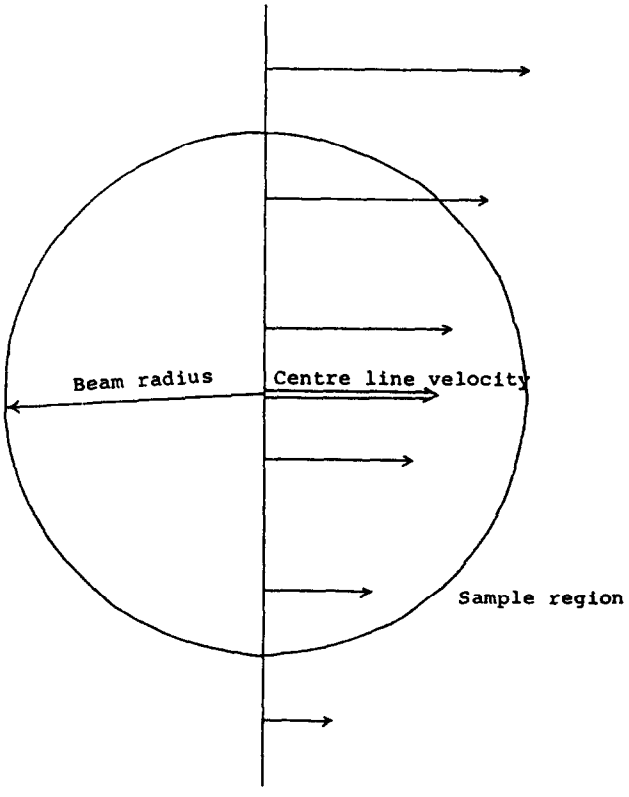

Fig 16. Geometry of the model used for simulating the effect of finite velocity gradients within the region of beam intersection.

The photon autocorrelation function is obtained by sampling this scattered light signal over a series of consecutive periods of time, each of length T_s (the "sample time"). If the number of photons detected in a sample time starting at time T is denoted by $n\ (T,\ T_s)$ then the autocorrelation function is formed by correlating the photon counts from samples separated by integral multiples of the same time i.e.

$$G^{(2)}(t) = \sum_T n(T,\ T_s)n(T+t,\ T_s) \tag{A2}$$

where t is the "channel delay time" and is an integral multiple of T_s. If the beam radius (r) is very large compared to the fringe spacing (s), then the time-dependent part of the correlation function can be approximated by [22]

$$G^{(2)}(t) = \frac{I_0}{u}\exp\left(\frac{u^2t^2}{r^2}\right)\left(\frac{1+w^2}{2}\cos\left(\frac{2\pi ut}{s}\right)\right) \tag{A3}$$

where w takes account of the reduced fringe contrast near the edges of the

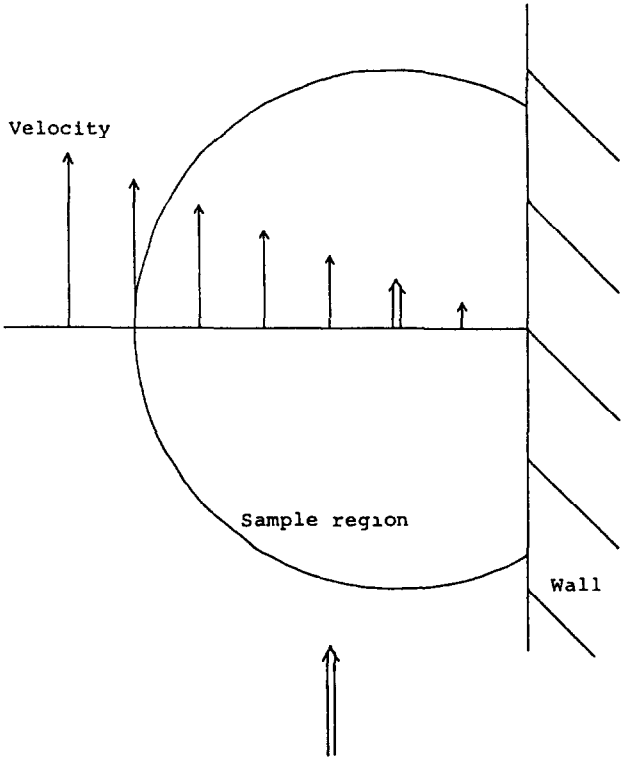

Fig 17 Geometry of the model used for simulating the effect of beam out off within the region of beam intersection

sample region. If the velocity is not constant over the whole sample region or over the duration of the sample, then the effect of the variation can be incorporated into the correlation function using

$$G^{(2)}(t) = \int_{-\infty}^{\infty} \rho(u) \exp\left(\frac{-U^2 t^2}{r^2}\right)\left(\frac{1+w^2}{2}\cos\left(\frac{2\pi u t}{s}\right)\right) du \tag{A4}$$

where $\rho(u)$ is the probability distribution function for the velocity. In general,

$$\int_{-\infty}^{\infty} \rho(u) du = 1. \tag{A5}$$

However in the example considered, where the velocity gradient in the sample region is treated as linear

$$\rho(u) = \frac{1}{u_2 - u_1}, \tag{A6}$$

where u_1 and u_2 are the lower and upper limits of the velocity in the sample region. Outside the range u_1 to u_2, $\rho(u) = 0$. In order to determine the effects of different velocity gradients across the slit, the integral A4 was evaluated numerically over a cylindrical sample region in Fig. 16 For the effects of a wall obscuring part of the sample region, the method shown in Fig. 17 was used. Although a parabolic velocity profile across the slit was considered, the velocity gradient in the sample region was assumed to be linear, and to take the value which was appropriate to the centreline of the sample region.